Tobias Schwinn, Lasath Siriwardena, Achim Menges

Integrative Agent-Based Architectural Design Modelling for Segmented Timber Shells

Abstract: Methods of planar re-meshing are an intensively studied topic in the fields of Architectural Geometry and Computer Graphics, which allow the design and eventual fabrication of double-curved shell structures from flat stock material. Planar hex-dominant (PH) meshes have vertex valence 3, a property that is important for the structural behavior of segmented timber shells. These shells are not only lightweight structures, but also offer additional benefits such as resource efficiency, low embodied carbon, and ease of prefabrication. Nevertheless, integrating architectural, structural, and fabrication constraints in the construction of PH-meshes remains a challenge, especially when transitioning from synclastic to anticlastic regions on a single design surface. Furthermore, state-of-the-art segmentation methods are largely inaccessible during early-stage architectural design. This paper presents an agent-based approach that addresses both the complex synclastic-anticlastic case and early-stage design usability. The model offers a novel conceptualization of timber shell segments as agents consisting of sub-agents representing segment vertices. We show how sub-agent-level decision-making and segment-level evaluation enables greater design flexibility and deeper integration of interdisciplinary constraints resulting in fairer segmentations than previous approaches. Real-world constraints from the realization of a multi-shell, large-scale segmented timber roof have informed method development thereby ensuring its applicability in design practice.

1 Introduction

Design, engineering, fabrication, and construction of segmented shells is a multi-facetted challenge addressed from multiple disciplinary perspectives. Recent research covers such diverse topics as design for assembly [1], segmentation methodology [2, 3], structural analysis [4], prefabrication and building system development [5] (Fig. 1), or extending the existing building stock through lightweight timber shells [6]. However, to successfully realize segmented shells, integrating disciplinary constraints in the design process is crucial. This paper consequently proposes a novel integrative approach for segmented shell design.

Shells are curved enclosing structures that are thin in relation to their span relying on ‘membrane action’ for structural stability [7]. The architectural relevance of shells lies in their ability to cover large areas column-free while using a minimal amount of material, and in their lightweight aesthetics where form and forces are inextricably

https://doi.org/10.1515/9783111162683-014

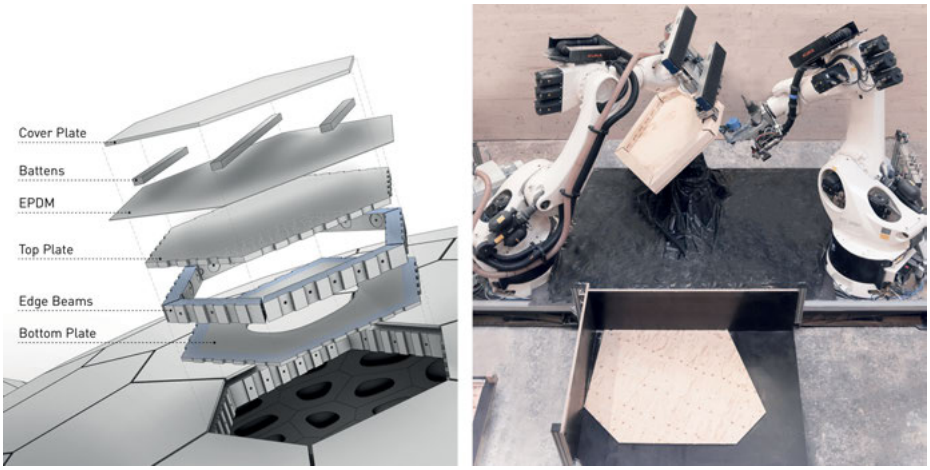

Fig. 1: Segmented timber shell building system of BUGA Wood Pavilion. Left: Exploded view of hollow cassette building system. Right: Robotic prefabrication of building system. Images: ©2019 University of Stuttgart.

linked. Segmented timber shells, besides being lightweight, can serve as carbon sinks, if designed for longevity and circularity.

Planar approximation methods for double-curved surfaces play an essential role in realizing segmented shells economically and ecologically. These methods allow construction from standard planar stock material, avoiding the need for custom molds or time-intensive milling. Furthermore, planar hex-dominant (PH) meshes, with most faces having 6-sides, exhibit architecturally relevant properties, such as vertex valence 3, a structurally stable configuration, where forces are translated between segments as normal and shear forces [8]; and, in contrast to triangular meshes, PH-meshes can be offset with constant thickness, where edges and faces remain parallel [9].

Constructing PH-meshes in architectural contexts requires considering geometric, structural, fabrication, assembly, aesthetic, and budgetary concerns. Constraints include the size of the available stock material in fabrication; size and weight limitations, when handling segments in assembly; and the joint pattern's structural and design implications. What makes the design of segmented shells a complex problem is that most of these evaluation criteria are intertwined, and changing one aspect will inevitably affect others. Despite substantial research into segmentation methods, constructing PH-meshes that integrate multi-disciplinary constraints remains a challenge—especially when transitioning from synclastic to anticlastic regions on a single design surface.

The contribution of this paper is an architectural design-oriented approach for free-form segmented timber shells that integrates constraints from all stakeholders involved in design, engineering, fabrication, and construction. The approach combines PH-meshing and agent-based modelling and offers a novel conceptualization of timber

shells as a system of agent systems. A case study validates its applicability in design practice in designing of a multi-shell, large-scale segmented timber roof under real-world constraints. The research offers valuable insights for the scientific community and industry by 1) proposing a systematic way for co-designing the segmentation under different disciplinary constraints; 2) providing direct control of segment shape and sizes in contrast to previous agent-based approaches; and 3) extending the accessibility of PH-meshing to the architectural design stages.

2 Related Work

PH meshing. Planar approximation of an arbitrary surface is a special case of remeshing based on selected criteria, which is an established research area in Computer Graphics (CG). It has specific applications in Architectural Geometry, including planar quad (PQ) meshing and planar hex-dominant (PH) meshing [9]. PH-meshing can be approached through Clustering, Tangent-Plane-Intersection (TPI), or "Dupin" methods.

Clustering methods, such as the ones proposed by Cutler and Whiting [10], generalize well, but result in unordered segmentations with heterogeneous segment sizes, edge lengths, and angles.

The simplest TPI method—also known as the 'apple-slicing' method [11]—addresses only the synclastic case. TPI methods based on the plate-lattice dualism [12], such as the one proposed by Troche [13], apply to both synclastic and anticlastic curvature cases and construct PH-meshes from the intersection points of tangent planes at the mesh vertices. While geometrically planar, the only available design variables are the distribution of vertices on the surface and the topology of the mesh, which limits the number of design criteria that can be applied to the segmentation. Zimmer et al. [14] consequently relaxed the tangency constraint, allowing more design freedom, and subjected the segmentation to optimization to achieve selected design goals. The main limitations of the TPI approach are the indirect control of plate properties, such as dimensions and edge lengths, as well as the challenge of transitioning from areas of positive to negative Gaussian curvature, the synclastic-anticlastic case, where intersection planes become almost co-planar.

Dupin methods share with the TPI methods the idea of a duality between triangle mesh and PH-mesh. Instead of generating planar plates directly, an intermediate non-planar dual mesh approximates the desired PH-mesh, which is optimized to minimize non-planarity. In this approach, "planar" consequently means "planar within tolerance", not truly planar as in the case of TPI. In the synclastic case, a non-planar barycentric dual of a triangular mesh suffices [15]. For anticlastic cases, the Dupin-indicatrix shapes the dual mesh based on surface curvature to produce an 'informed' dual mesh [16]. Further development uses the conjugate curve network of principal curvature lines to generate a shifted quad layout as the basis for optimization [17].

The most computationally advanced methods for creating PH-meshes fall into the Dupin category, resulting in ordered, principal curvature-aligned segmentations that 'naturally' follow the principal curvatures in the shell surface. However, the non-linear optimization involved goes beyond industry-standard Computer-Aided Geometric Design (CAGD) software. The first research objective therefore is to develop accessible methods for the design of segmented shells based on the duality approach and to validate them in a case study.

Agent-based Design of Segmented Timber Shells. Agent-based modelling and simulation (ABMS) is a numerical method for modelling and simulating complex systems that is used in various fields including architectural design, engineering, and construction (AEC) [18]. In ABMS, a segmented shell is considered a system of interacting agents that implement segment generation while pursuing their own objectives. Since 2014, two of the above methods have been implemented through ABMS and used to design and fabricate two segmented timber shells.

In the Landesgartenschau Exhibition Hall (Fig. 2, left), which spans 11 m, agents represent solid Beech plywood plates generated through TPI on a design surface with both synclastic and anticlastic regions [19]. In the BUGA Wood Pavilion for the Bundesgartenschau 2019 (Fig. 2, right), agents represent hollow cassettes generated through the 'apple-slicing' method on a synclastic design surface [20]. These cassettes consist of top and bottom plates connected by edge beams (Fig. 1), allowing for a span of close to 30 m with a similar weight-area ratio as the Landesgartenschau shell. The related ABMS innovation is the conceptualization of plate edges as sub-agents that steer their plate's tangent plane.

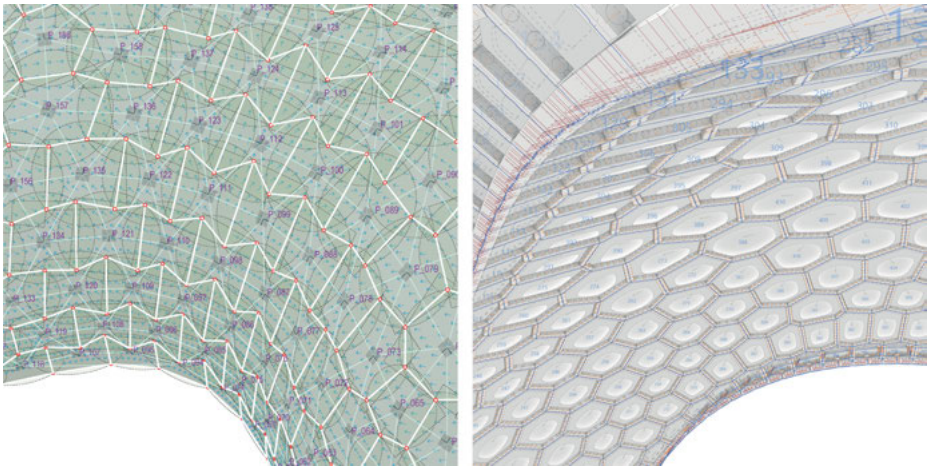

Fig. 2: Agent-based design of segmented shells. Left: Single-layer solid timber plates of Landesgartenschau Exhibition Hall 2014. Right: Double-layer hollow cassettes of BUGA Wood Pavilion 2019. Images: ©2014, 2019 University of Stuttgart.

These projects showed that ABMS effectively addresses the problem of indirectly controlling plate outlines by managing the complexity of iterative repositioning of tangent planes and subsequent remodeling of plate outlines for large segmentations. They also showed that ABMS enables the integration of later-stage AEC constraints into the early design process, significantly influencing segmentation. The BUGA project showcased that segments composed of sub-elements can lead to much higher performing structures despite increased fabrication complexity. However, current agent-based implementation rely on TPI methods and their associated limitations. The second research objective therefore is to develop a Dupin-based agent model to avoid the strict tangency constraint thereby expanding the capabilities of ABMS in segmented shell design.

3 Methods

To address the second research objective, we conceptualize a segmented timber shell as a system of agents representing a planar segments called plates. Each plate is defined by a group of sub-agents representing its vertices. In line with the Dupin approaches mentioned above, the segmentation of the design surface S is based on an "ideal" triangulation M, which is aligned with the principal curvature directions. The minimum principal curvature lines running through the umbilical points of S act as spines from which the two sets of principal curvature (PC) lines are constructed using the Runge-Kutta (RK4) method [21] (Fig. 3, left). The intersections of these PC lines form the vertices of the primal mesh M. The dual mesh D is generated for each vertex in M using barycenters of the adjacent faces (Fig. 3, center). D then initializes the agent system, which computes planar segments meeting given design constraints (Fig. 3, right).

3.1 Agent System

Agent systems typically consist of three main system constructs: agents, their behaviors, and the environment in which the agents interact [18]. Each plate agent represents a mesh face of the dual mesh D, with coincident vertices as vertex agents (Fig. 4, left). Edges in D indicate interaction topology, whereby every vertex agent is connected to at least two, typically three, others. Adjacent closed loops indicate segment membership, with every vertex agent being a member of up to three plate agents (Fig. 4, right). Vertex agents at the perimeter of a shell, i. e., the 'naked' vertices of D are considered anchors by default. Plate agents that accommodate a column head or technical equipment, such as smoke vents, at system initialization can be flagged accordingly. Figure 4 illustrates the specific attributes defining agent types and states.

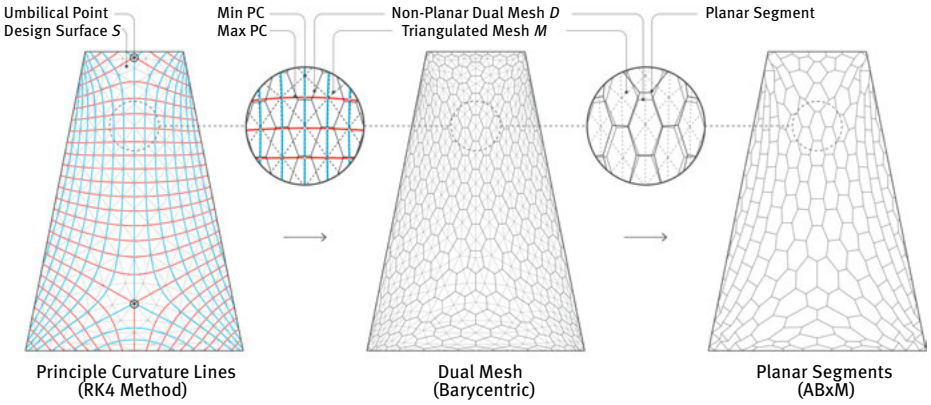

Fig. 3: Steps of segmentation process. Left: Generation of primal triangle mesh. Center: Generation of polygonal dual mesh. Right: Constraint-based planarization of segments.

Consequently, a vertex agent's environment is defined by the states of neighboring vertex agents, its parent agents, as well as base surface properties such as local curvature. Vertex agents iteratively update their states based on their internal states and the state of their environment, using goal-oriented behaviors. The resulting model is a hierarchical network-based agent system, with decision-making and action occurring at the of sub-agent level and evaluation at the segment-level.

3.2 Agent Behaviors

According to Levitis et al. [22], behaviors are the internally coordinated response (action or inaction) of whole entities to internal or external stimuli. Defining a behavior from a system modeler's point of view thus means providing the rules for the internal computation that leads, in our case, to a change of location of vertex agents such that the plate agent approaches its desired state. This translation $\mathbf{v}$ w.r.t. the current location of a vertex agent takes the fundamental form of

$$\mathbf{v} = \alpha \cdot \frac{1}{N} \cdot \sum_{i=1}^{N} (P_i - P_a)\,, \text{ with } 0 < \alpha \leq 1 \tag{1}$$

where α is a user-defined scaling factor controlling the resultant step size, N is the number of neighbor agents, P_i the target point computed by the current behavior w.r.t the neighbor agent i, and P_a is the current position of the vertex agent. In the following, we describe the rules to achieve six design objectives related to geometry, architecture, fabrication, technical systems, and structure.

Planarity behavior (PL). This geometrical behavior aims to achieve planarity of the plate polyline by minimizing the cumulative distance of the plate vertices to the fitplane. The target point P_i is the closest point on the frame of adjacent plate agent i.

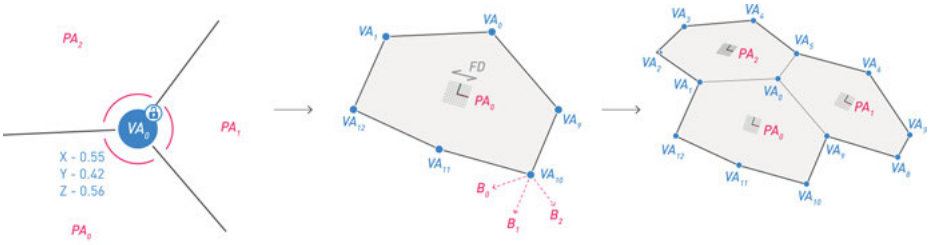

VertexAgent	
Position	Cartesian coordinates
IsAnchor	Anchor Flag
IsMemberOf	List of PolyAgent IDs
HasUpdated	Modification Flag

PolyAgent	
VertexAgents	List of VertexAgent IDs
Frame	Fit-Plane of Vertices
Polyline	Outline of Plate
Centroid	Vertex Average
Fibre Vector	Grain Direction
Area	Project Area on Frame
IsColumn	Column Flag
IsVent	Contains Vent Flag
Behaviors	Behaviors for vertex agents to update states to reach a specified goal

PolyAgent System	
PolyAgents	List of PolyAgent IDs
Total Displacement	Cumulative Translation of all Vertices
Threshold	System Convergence Value based on Total Displacement

Fig. 4: Agent system constructs. Left: Vertex Agent. Center: Plate Agent. Right: Agent system.

Every vertex agent will compute up to 3 different target points P_i, one for each plate that it belongs to, and will average its resultant translation vectors (Fig. 5, top left).

Surface Approximation behavior (SA). This design behavior aims to closely approximate the base surface by minimizing 1) the distance between the plate agent's centroid and the closest point on the surface P_c and 2) the angular distance between the agent's Frame orientation and the surface normal at P_c. First, a proxy frame $F_{px,i}$ of plate agent i is calculated:

$$F_{px,i}(P, N) = \alpha \cdot (T_{pc,i} - F) \tag{2}$$

where $T_{pc,i}$ is the tangent plane at P_c and F_i is the i-th plate agent's frame. Then, the target point P_i is the closest point on the proxy frame $F_{px,i}$. Like PL, every vertex agent will compute up to 3 different target points P_i (Fig. 5, top right).

Plate width behavior (PW). This fabricational behavior aims to limit the width of the bounding rectangle, which encloses the plate polyline, to a maximum user-defined value to ensure fabricability. This value will usually correspond to the dimensions of a chosen stock material, such as 3-ply or CLT. If the bounding rectangle is larger than the user-defined value, the target point Pi of the current vertex agent is the centroid of plate agent i, effectively shrinking the plate (Fig. 5, center left).

Plate area behavior (PA). This technical behavior aims to ensure a minimum surface area of the segment, e. g, to allow technical systems to be embedded in selected plates. This behavior operates in the opposite way of the PW behavior in that the target point P_i

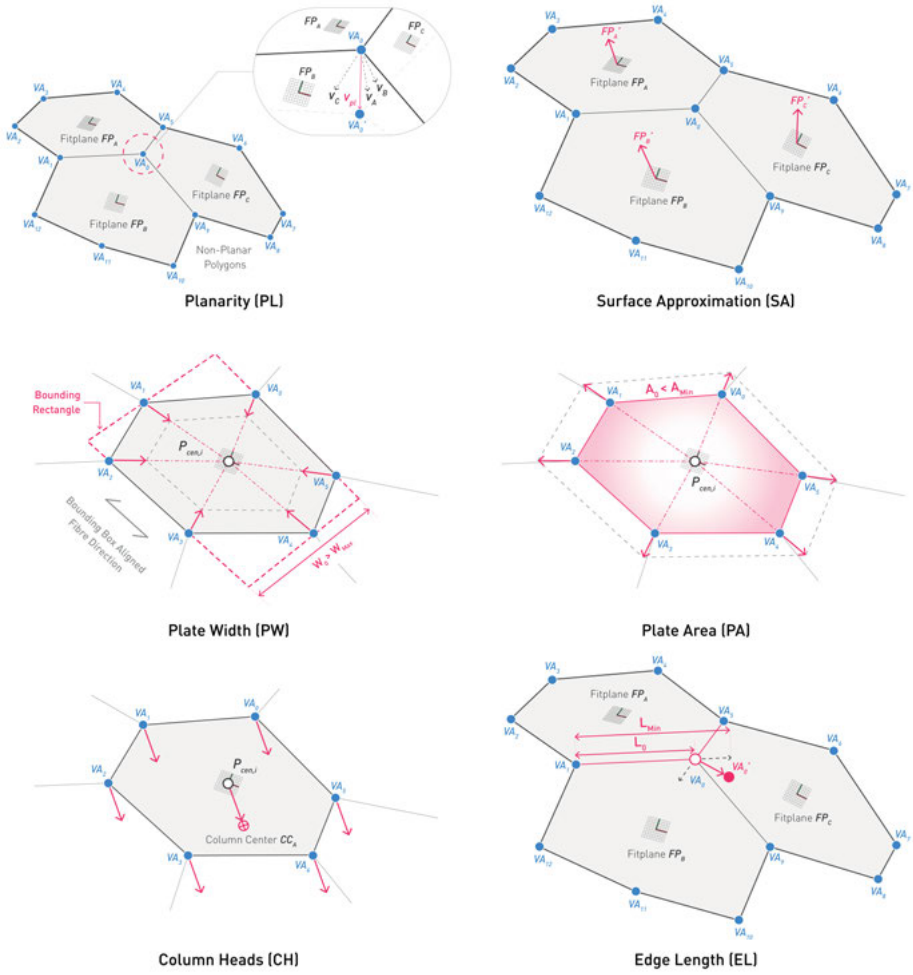

Fig. 5: Plate Agent Behaviors. Planarity, Surface Approximation, Plate Width, Plate Area, Plate Column Head, and Plate Edge Length.

of the translation lies in the opposite direction to the centroid of plate agent *i* effectively increasing the size and area of the plate up until a user-defined minimum area target value is met (Fig. 5, center right).

Column heads behavior (CH). This structural behavior aims to ensure that a segment flagged as having a column will be roughly centered on the column head to avoid eccentricity. The target point P_i is the column head associated with plate agent *i* (Fig. 5, bottom left).

Edge length behavior (EL). This structural behavior aims to enforce a given minimum edge length to make sure loads can be transferred across the edge via a minimum

amount of crossing screw pairs. If the current vertex agent is closer than a user-defined minimum distance value to its neighbor vertex agent i, then the target point P_i of the translation lies in the opposite direction to vertex neighbor i (Fig. 5, bottom right).

Resulting translation. The behaviors described above will compute up to six individual translation vectors for each vertex agent. The resultant translation $\mathbf{v}_t$ of a vertex agent is the weighted average of all its behaviors:

$$\mathbf{v}_t = \frac{w_{\mathrm{pl}} \cdot \mathbf{v}_{\mathrm{pl}} + w_{\mathrm{sa}} \cdot \mathbf{v}_{\mathrm{sa}} + w_{\mathrm{pw}} \cdot \mathbf{v}_{\mathrm{pw}} + w_{\mathrm{pa}} \cdot \mathbf{v}_{\mathrm{pa}} + w_{\mathrm{ch}} \cdot \mathbf{v}_{\mathrm{ch}} + w_{\mathrm{el}} \cdot \mathbf{v}_{\mathrm{el}}}{w_{\mathrm{pl}} + w_{\mathrm{sa}} + w_{\mathrm{pw}} + w_{\mathrm{pa}} + w_{\mathrm{ch}} + w_{\mathrm{el}}} \tag{3}$$

where w_{pl}, w_{sa}, w_{pw}, w_{pa}, w_{ch}, and w_{el} are user-defined weight parameters. As demonstrated in previous work, those parameters can be subject to parameter optimization to minimize a certain score, such as the number of iterations to convergence or a measure of the segmentation quality [3].

3.3 Implementation

The model described in Sec. 3.1 and 3.2 is implemented in C# using an object-oriented approach as an extension to the agent-based modelling framework ABxM [23]. Custom agent and behavior classes are derived from the framework's base classes. The vertex agent class is derived from the Cartesian agent class, which allows for position-based modelling and faster convergence than previous force-based approaches. System updates are performed iteratively and synchronously to ensure consistency between agent updates within each iteration.

To address the first research objective, 1) the source code and UML diagram of this implementation is published open access [24]; and 2) ABxM is an addon to the popular CAGD software environment Rhinoceros 3d and is available through its package manager. Implementing the model in a widely used software environment increases accessibility and ensures that the approach can be part of a larger design-to-fabrication workflow as demonstrated in the following case study.

4 Large-Scale Construction Robotics Laboratory

The research described above was conducted as part of the design of the Large-Scale Construction Robotics Laboratory (LCRL) for the Cluster of Excellence "Integrative Computational Design and Construction for Architecture" (IntCDC) in Stuttgart, Germany. The roof design of the LCRL building thus serves as a case study and validation of the modelling approach.

4.1 Project Description

The LCRL is a three-story laboratory building serves as a demonstrator for IntCDC's research. It features a column-free 1415 m^2 testing hall and a 3200 m^2 timber roof covering the entire structure, including offices and workshops (Fig. 6). Unlike prior segmented timber shells, the shell is integrated into a full-scale building, hovering 10 m above ground, and is only point supported. The roof consists of seven trapezoidal shells, spanning 28.8 m, that roughly form barrel vaults and transition between synclastic and anticlastic curvature regions at their corners (Fig. 7). These shells address additional constraints such as interfacing with timber columns, the facade, solar panels, fire vents, HVAC systems, and a fibre-reinforced skylight above the office section. The roof is expected to be completed in Q3 2025.

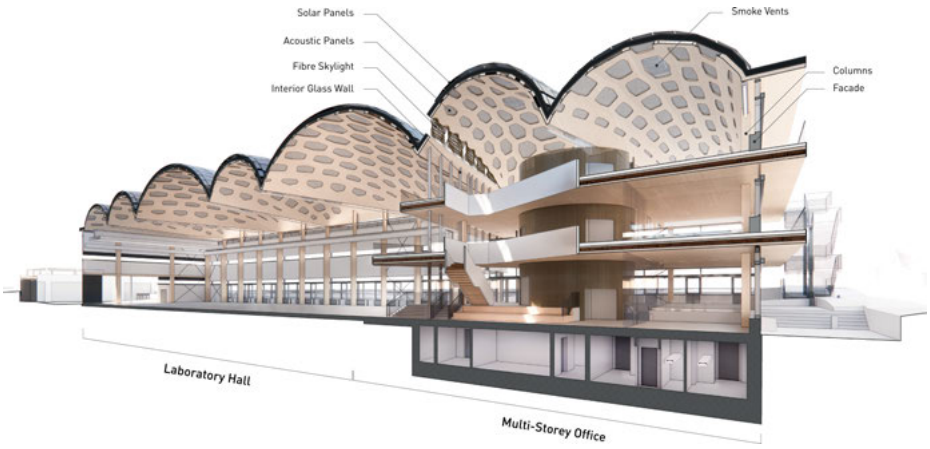

Fig. 6: Section view of the case study Large-scale Construction Robotics Laboratory (LCRL).

4.2 The Workflow

The segmented shells of the LCRL are designed using a workflow that includes 1) modelling of a design surface, 2) segmentation, and 3) evaluation of the segmentation based on AEC criteria.

Surface Design. The goal is to create a shell surface S that adapts to boundary constraints such as support positions. Lofting five G2 curves yields a NURBS surface, which acts as an interim surface. This interim surface is then 'inflated' via vertex normal displacement to increase mean curvature, optimizing structural and material efficiency. A parameter study facilitates preliminary structural optimization, leading to a structurally informed free-form design surface S.

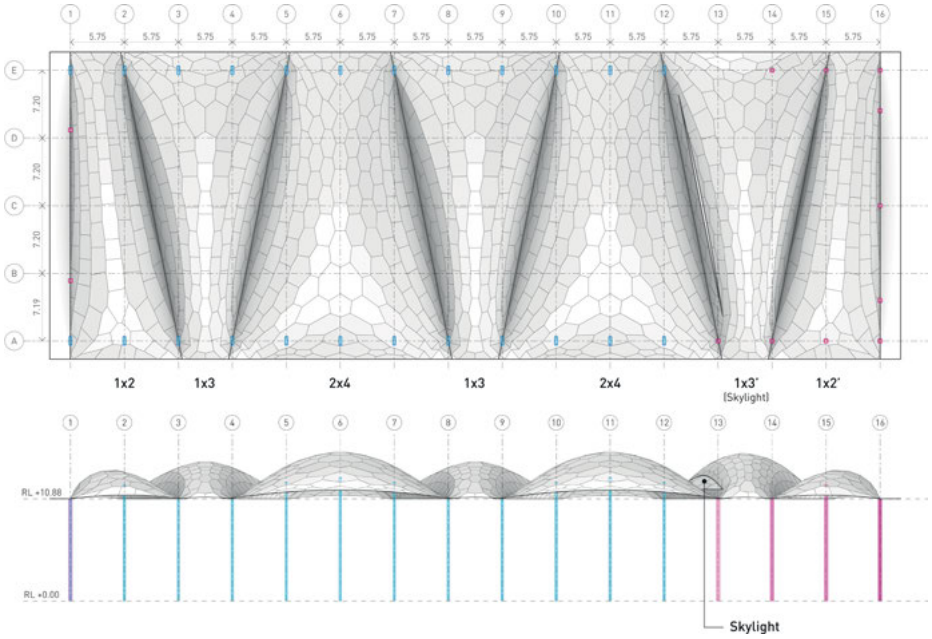

Fig. 7: Plan and Elevation of LCRL Roof.

Segmentation. In this step, the agent-based segmentation method described above is used (Fig. 3) including the creation of a PC-aligned mesh M from S and its transformation into a non-planar dual mesh D initializing the agent system.

The project-specific constraints applied in the case study include achieving segment planarity within a tolerance of 0.1 mm, approximating surface S, limiting the fiber-aligned plate width to 2.35 m (based on sheet sizes of 2.5×6.0 m), ensuring a minimum surface area of 6 m^2 for vent segments, centering column segments around the column head, and maintaining edge lengths larger than 0.3 m. M is produced using a custom mesher incorporating additional vertex points near the umbilical points that deviate from the PC lines, to avoid large changes in segment sizes between neighboring plates. Considering the anisotropic properties of timber, the fiber direction of the segments is aligned with the principal stress direction in the segments.

Evaluation. Each segment is continuously evaluated at runtime w.r.t. constraints that have been defined locally in the agent behaviors. After convergence, the resultant segmentation is also evaluated w.r.t. to global design criteria (Fig. 8). These include:

Structural evaluation to compute deflection, utilization, segment type (massive vs. hollow), material selection, and fibre direction. Massive cassettes are necessary in areas of high stress concentrations around the column heads. Structural criteria generally aim for reducing the number of segments, i. e., having bigger segments to

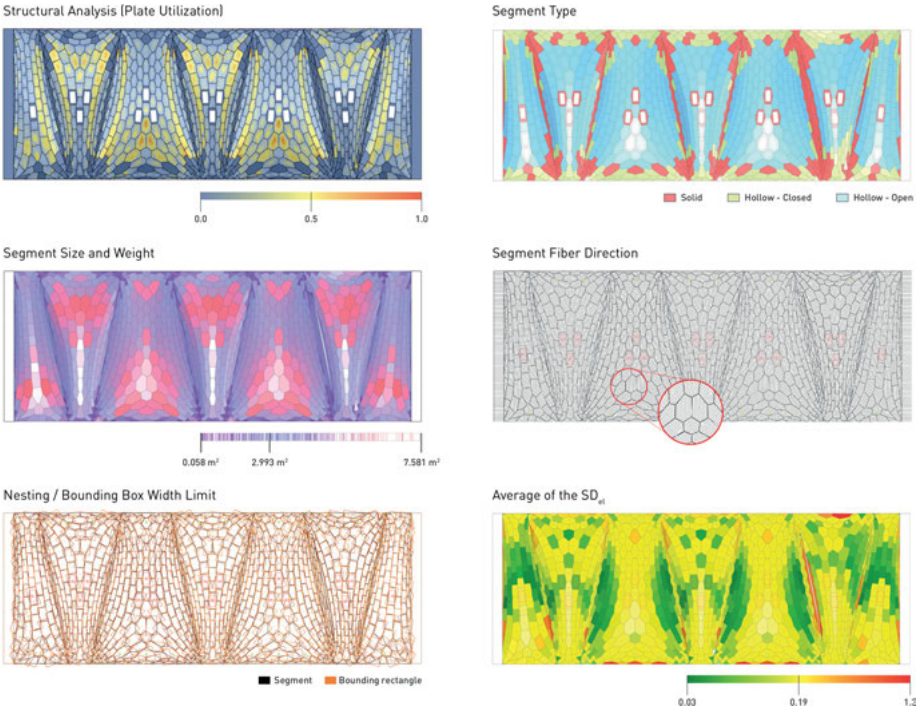

Fig. 8: Evaluation of LCRL Roof. Left-to-right, top-to-bottom: structural, solid vs hollow, size and weight, fibre direction, nesting/bounding box width limit, Distribution of fairness values of the SD_{el} centered on median value of 0.19 (yellow).

reduce global deflection. Limits are imposed by stock size availability and producibility (robot payload and reach).

Fabrication analysis evaluating robotic producibility w.r.t. fibre-aligned segment sizes (nesting), segment weight (payload), number of elements, fabrication steps, and expected fabrication time.

Cost analysis considering number and types of segments, build-up, and nesting efficiency using unit prices provided by the manufacturer as a reference. These factors heavily influence material usage and assembly time on-site and off-site and therefore cost estimates.

Interfacing with column heads and smoke vents is evaluated at run-time, while interfacing with the facade, is evaluated after convergence. During concept design, the evaluation is based on qualitative criteria such as connection complexity and presumed ease of production.

Architectural evaluation assessing the fairness of the segmentation. Fairness is defined by the angle between plates (avoiding sharp kinks for visual reasons and to minimize stress concentrations), the interior angle of plates, and the standard deviation of edge lengths SD_{el} to indicate regularity [3].

4.3 Results

The evaluation of different segmentations and comparing design options in terms of cost and structural performance are crucial for decision-making (Tab. 1). During concept and schematic design stages (HOAI stages 2 and 3), four of the many design iterations of the roof have been evaluated accordingly in collaboration with a manufacturer as part of a pre-construction agreement. Option 1, with a total of 1175 segments, is the first segmentation that has been fully analyzed and priced. It has a wide range of segment sizes, some exceeding the available stock sizes. It also exceeded the permissible structural utilization. Consequently, Option 2 was generated, specifically considering segment widths and adjusting the segment buildup. Options 2 and 3 are identical segmentations with 1128 segments but differ in terms of fibre orientation and consequently the distribution of massive and hollow cassettes. Option 4, with 1262 segments, aimed to reduce plate sizes further but increased deflections and localized stresses due to the increased number of segments and joints.

Tab. 1: Design options. Material options are Cross-Laminated-Timber (CLT), 3-ply (3P), Glulam beams (GL), and Laminated Veneer Lumber (LVL). Unit price of hollow cassettes includes costs for buildup and pressing, but no insulation, waterproofing, and cladding. (*) Max. deflection value in this option is not comparable due to different segment stiffness assumptions.

	Opt. 1	**Opt. 2**	**Opt. 3**	**Opt. 4**
No. segments	1175	1128	1128	1262
No. of massive	463	440	380	398
No. of hollow	712	688	748	864
Total Area	3240.1	3274.3	3216.4	3357.8
Massive cassettes				
Massive area	701.2	826.4	718.7	616.7
Buildup massive	CLT	CLT	CLT	CLT
Max. width (m)	2.9	2.4	2.4	2.35
Max. weight massive (kg)	855.6	694.0	694.0	600.0
Unit price change per m^2 (%)	100.0	88.9	88.9	88.9
Hollow cassettes				
Hollow area	2538.9	2549.9	2657.6	2741.1
Buildup hollow	3P/GL/3P	3P/GL/LVL	3P/GL/LVL	3P/GL/LVL
Max. width (m)	2.9	2.4	2.4	2.35
Max. weight hollow (kg)	348.0	326.3	326.6	298.00
Unit price change per m^2 (%)	100.0	106.5	105.7	107.4
Total len. edge beams (m)	5440.3	5802.6	5802.6	6277.3
Total len. screw edge (m)	3698.2	3684.4	3684.4	3934.00
Nesting efficiency (%)	58.4	56.6	59.2	60.2
Max. deflection (mm)	–*	–102	–94	–106
Structural utilization (top plate)	>1.0	<1.0	<1.0	<1.0
Average SD_{el}	0.299	0.319	0.319	0.306

Fig. 9: Interior view of the LCRL hall covered by the segmented timber roof.

Within the evaluation process, nesting efficiency emerges as a critical metric. Considering the size of the roof, the 2.6 % increase in nesting efficiency between Options 2 and 3 corresponds to a material saving of 262.2 m^2. To further increase material utilization, we aim to use offcut not suitable for roof plates as façade material. Based on these findings, Option 3 was chosen for further development in detail design (Fig. 9).

5 Discussion and Conclusion

In the case study, we successfully showed how 'real-world' constraints of the design of a large spanning roof can be integrated into the segmentation process and inform design decisions, thereby addressing our first research objective. Our main finding relates to our second objective: a plate system where plate vertices are conceptualized as sub-agents of plate agents allows for more detailed control of the final segmentation with respect to defined performance criteria than previous approaches—most notably TPI and black-box algorithms.

While the conceptualization of segments as agents makes it easier to formulate modelling goals, it still requires specialist training to be able conceptualize and model a system from the bottom up. Furthermore, the behaviors that we have implemented are only a subset of rules that can be imagined and implemented. This means that we cannot guarantee that we have identified the optimal behaviors to achieve the desired goals, which is a main limitation of metaheuristic approaches. Reinforcement learning has shown promising results for defining behavioral rulesets without preconceived rules of thumb [3].

A limitation of our approach is that the triangulation is not part of the agent-based approach, which means that changing the interaction topology by the agents themselves is currently not possible. In further work, we will therefore aim to integrate the curvature-aligned triangulation into the agent-based architectural modelling approach for segmented timber shells. Furthermore, additional evaluation criteria like carbon modeling need to be integrated into the post-convergence evaluation of the agent system.

Acknowledgements

This research has been supported by the Deutsche Forschungsgemeinschaft (DFG) under Germany's Excellence Strategy – EXC 2120/1 – 390831618.

We would also like to thank the architects and engineers of the IntCDC Planungs-GmbH, particularly Moritz Münzenmaier and Daniel Sonntag, for the design, analysis, and coordination of the LCRL building into which we can integrate our research.

References

[1] G. T.-C. Kao, A. Iannuzzo, B. Thomaszewski, S. Coros, T. Van Mele, and P. Block. 2022. Coupled rigid-block analysis: stability-aware design of complex discrete-element assemblies, *Computer-Aided Design,* 146, 103216, DOI: 10.1016/j.cad.2022.103216

[2] K. Pluta, M. Edelstein, A. Vaxman, and M. Ben-Chen. 2021. PH-CPF: Planar Hexagonal Meshing using Coordinate Power Fields, *ACM Trans. Graph.* 40(4), DOI: 10.1145/3450626.3459770

[3] T. Schwinn. 2021. A Systematic Approach for Developing Agent-based Architectural Design Models of Segmented Shells: Towards Autonomously Learned Goal-oriented Agent Behaviors, PhD, University of Stuttgart, DOI: 10.18419/opus-11633

[4] S. Bechert, D. Sonntag, L. Aldinger, and J. Knippers. 2021. Integrative structural design and engineering methods for segmented timber shells – BUGA Wood Pavilion, *Structures,* 34, 4814–33, DOI: 10.1016/j.istruc.2021.10.032

[5] H. J. Wagner, M. Alvarez, A. Groenewolt, and A. Menges. 2020. Towards digital automation flexibility in large-scale timber construction, *Constr. Robot.,* 4(3–4), 187–204, DOI: 10.1007/s41693-020-00038-5

[6] A. Groenewolt. 2023. Timber Plate Structures as a Roof Construction System, Doctoral Thesis, Institute for Computational Design and Construction, Stuttgart.

[7] Art & Architecture Thesaurus Online, Shell Structures. http://vocab.getty.edu/aat/300001276

[8] R. La Magna, F. Waimer, and J. Knippers. 2012. Nature-inspired generation scheme for shell structures, In *Proceedings of the International Association for Shell and Spatial Stuctures (IASS) Symposium,* Seoul, Korea. http://d-nb.info/1051812577/34

[9] H. Pottmann, M. Eigensatz, A. Vaxman, and J. Wallner. 2015. Architectural geometry, *Comput Graph* 47, 145–64, DOI: 10.1016/j.cag.2014.11.002

[10] B. Cutler and E. Whiting. 2007. Constrained planar remeshing for architecture, In *Proceedings of Graphics Interface 2007,* ACM Press, p. 11. DOI: 10.1145/1268517.1268522

[11] A. Bagger. 2010. Plate shell structures of glass Studies leading to guidelines for structural design, Dissertation, Technical University of Denmark.

[12] T. Wester. 1989. Design of Plate and Lattice Structures Based on Structural Dualism, In *Proceedings of the IASS Annual Symposium 1989,* Madrid.

[13] C. Troche. 2008. Planar Hexagonal Meshes by Tangent Plane Intersection, In *Advances in Architectural Geometry 2008,* Vienna, pp. 57–60.

[14] H. Zimmer, M. Campen, R. Herkrath, and L. Kobbelt. 2012. Variational Tangent Plane Intersection for Planar Polygonal Meshing, In *Advances in Architectural Geometry 2012,* pp. 319–32. DOI: 10.1007/978-3-7091-1251-9_26

[15] C. Robeller and N. Von Haaren. 2020. Recycleshell: Wood-only Shell Structures Made From Cross-Laminated Timber (CLT) Production Waste, *Journal of the International Association for Shell and Spatial Structures,* 61(2), 125–39, DOI: 10.20898/j.iass.2020.204.045

[16] W. Wang and Y. Liu. 2009. A Note on Planar Hexagonal Meshes, In *Nonlinear Computational Geometry,* I. Z. Emiris et al., Eds., The IMA Volumes in Mathematics and its Applications, vol. 151. New York, NY: Springer, pp. 221–33. DOI: 10.1007/978-1-4419-0999-2_9

[17] Y. Li, Y. Liu, and W. Wang. 2015. Planar Hexagonal Meshing for Architecture, *IEEE Trans. Vis. Comput. Graph.,* 21(1), 95–106, DOI: 10.1109/TVCG.2014.2322367

[18] D. Stieler, T. Schwinn, S. Leder, M. Maierhofer, F. Kannenberg, and A. Menges.2022. Agent-based modeling and simulation in architecture, *Automation in Construction* 141, 104426, DOI: 10.1016/j.autcon.2022.104426

[19] T. Schwinn, O. D. Krieg, and A. Menges. 2014. Behavioral Strategies: Synthesizing design computation and robotic fabrication of lightweight timber plate structures, In *Design Agency,* Los Angeles, pp. 177–88. DOI: 10.52842/conf.acadia.2014.177

[20] A. Groenewolt, T. Schwinn, L. Nguyen, and A. Menges. 2018. An interactive agent-based framework for materialization-informed architectural design, *Swarm Intelligence,* 12(2), 155–86, DOI: 10.1007/s11721-017-0151-8

[21] D. Rutten and S. Gregson. 2011. Principal curvature lines on surfaces, *Grasshopper3d Forum.* https://www.grasshopper3d.com/xn/detail/2985220:Comment:1486232 (May 25, 2023).

[22] D. A. Levitis, W. Z. Lidicker, and G. Freund. 2009. Behavioural biologists do not agree on what constitutes behaviour, *Anim. Behav.* 78(1), 103–10, DOI: 10.1016/j.anbehav.2009.03.018

[23] L. Nguyen et al. 2022. ABxM.Core: The Core Libraries of the ABxM Framework, *DaRUS,* DOI: 10.18419/darus-2994

[24] T. Schwinn et al. 2023. ABxM.PlateStructures: Agent-based Architectural Design of Plate Structures, *DaRUS,* DOI: 10.18419/darus-3438